

*Full Length Research Paper*

# Photocatalytic activity of nanopolyaniline (NPA) on phenol degradation

Tesfa Oluma Fufa\*, Abi Tadesse Mengesha and Om Prakash Yadav

Chemistry Department, Haramaya University Post Box: 138, Dire Dawa, Ethiopia.

Received 30 April, 2016; Accepted 15 July, 2016

**Nanopolyaniline (NPA) has been synthesized by chemical oxidative polymerization of aniline and characterized using Fourier transmission infrared (FTIR), X-ray diffraction (XRD) and ultra-violet visible techniques. XRD patterns confirm that NPA has crystallite size of 37 nm with monoclinic structure and UV-visible spectra indicate its band gap energy is 1.96 electron volts. Photocatalytic efficiency of as-synthesized NPA was studied using degradation of phenol as a probe. Effects of photocatalyst load, pH and phenol initial concentration on the degradation of phenol were investigated. Using phenol initial concentration (50 mg L<sup>-1</sup>) and optimum photocatalyst load (200 mgL<sup>-1</sup>) and pH 10, degradation of phenol at 3 h was 93.5%. Degradation of phenol follows first order kinetics with rate constant (k) 1.62×10<sup>-2</sup> min<sup>-1</sup>.**

**Key words:** Degradation, photocatalytic efficiency, polyaniline, phenol, X-ray diffraction (XRD).

## INTRODUCTION

Phenol (C<sub>6</sub>H<sub>5</sub>OH) is a natural as well as an artificial organic compound (Azni and Katayon 2002; Khazi et al., 2010; Guido et al., 2008). It is slightly acidic, but requires careful handling due to its propensity to cause burns. Industrially, phenol is manufactured to synthesize many items: Phenolic resins, plastics, explosives, fertilizers, paints, rubbers, textiles, adhesives, drugs, papers, soaps, etc.

Phenol discharged into environment during its production or application is a major source of water contamination due to its toxicity and non-biodegradable nature (Liotta et al., 2009; Mohammad et al., 2012). Overexposure of human being to phenol causes severe injuries to liver, kidney, lungs and vascular system

(Shawabkeh et al., 2010; Al-Khasman, 2010). As set by Environmental Protection Agency, the maximum permissible limit of phenol in drinking water is 4 mg L<sup>-1</sup> (Shawabkeh et al., 2010; Al-Khasman, 2010). Various technologies involving physical (Sun et al., 2011), biological (Basha et al., 2010; Guido et al., 2008; Khazi et al., 2010) and chemical methods (Arjunan and Karuppa 2011) have, earlier, been reported to minimize the concentration of phenol in polluted water. These methods are not advantageous, since they simply transfer pollutants from one phase to another and generate solid waste that requires secondary treatment. Advanced oxidative process (AOP) involving photo-catalysis is an

\*Corresponding author. E-mail: tesfaolumaf@gmail.com. Tel: +251933257514.

efficient, cost effective and clean method for the treatment of water contaminated with organic pollutants prevention (Yan and Sun, 2007; Tao et al., 2012). This process is based on the generation of the strongly oxidizing hydroxyl radicals ( $\cdot\text{OH}$ ), which oxidizes many organic pollutants that could be present in water.

Photo-catalysis involving light induced semiconductor activation has received remarkable attention because of its potential application in the conversion of light energy into chemical energy and environmental pollution control (Kiros et al., 2013; Alebel et al., 2015; Achamo and Yadav, 2016). Among AOPs, heterogeneous photo-catalysis exhibits better efficiency for degrading many organic contaminants into  $\text{CO}_2$ ,  $\text{H}_2\text{O}$  and some biodegradable mineral acids (Tesfay et al., 2013; Marshet et al., 2015). To promote adsorption of substrates on photocatalyst surface and facilitate generation of hydroxyl radicals, it must be improved by rapid charge separation, surface acidity/alkalinity and  $\text{OH}^-$  group surface population.

To carry out a photochemical change, charge transfer reaction must compete efficiently with the electron-hole recombination process that takes place within nanosecond. Due to this rigorous reaction, pre-adsorption of charge trapping species ( $e^-$  acceptors,  $\text{O}_2$  and  $e^-$  donors like  $\text{H}_2\text{O}$ ) are assumed to lead efficient chemical reactions. Sunlight spectrum consists of UV (7 %), visible light (46%) and infra-red (47%) (Bak et al., 2002). Thus, in the recent years, major research focus has been on exploring visible light active photocatalysts.

Semiconductor polymers such as polyaniline, polypyrrole, polythiophene and polyacetylene have been of interest in photo-catalysis fields (Salaices et al., 2004; Ali et al., 2007). Polyaniline due to its ease of preparation, low cost, better electronic and optical properties, high conductivity and excellent environment stability, has a number of applications such as in electromagnetic interference shielding, rechargeable batteries, chemical sensors, corrosion devices, microwave absorption and photo-catalysis. Its efficient photo-generated  $h^+$  transporting ability can facilitate the separation of  $e^-$ - $h^+$  pairs (Srinivas et al., 2012). This study is aimed to study the photo-catalytic activity of as-synthesized nanosize-polyaniline photo-catalyst for degrading phenol dissolved in water under irradiation of artificial visible light. Influence of operational parameters: photocatalyst load, solution pH, phenol initial concentration and irradiation time. Photo-catalytic degradation mechanism over nanopolyaniline (NPA) has also been discussed in detail.

## EXPERIMENTAL

### Chemicals

Aniline ( $\text{C}_6\text{H}_5\text{NH}_2$ ; MW = 93.13  $\text{g mol}^{-1}$ ; FLUSKA), ammoniumper-sulphate [ $(\text{NH}_4)_2\text{S}_2\text{O}_8$ ; MW = 228.18  $\text{g mol}^{-1}$ , BDH chemicals], hydrochloric acid (HCl, MW = 36.46  $\text{g mol}^{-1}$ ; FLUSKA) and sodium hydroxide ( $\text{NaOH}$ , 40.0  $\text{g mol}^{-1}$ ; Blulux, Laboratory).

### Synthesis of nanopolyaniline (NPA)

The NPA was synthesized by chemical oxidative polymerization method (Gospodinova and Terlemezyan, 1998; Shukla et al., 2010; Hirotsugu and Hiromasa, 2011; Srinivas et al., 2012). Typically, 2M aniline ( $\text{C}_6\text{H}_5\text{NH}_2$ ) and 2M ammoniumpersulphate [ $(\text{NH}_4)_2\text{S}_2\text{O}_8$ ], each prepared in 1 M HCl solution, were mixed in a beaker and by magnetically stirred for 1 h and kept at room temperature for 12 h. The polymer thus formed was filtered out, washed with de-ionized water, and dried at 60°C in oven for 30 min. The product was milled using mortar and pestle and finally kept in a moisture-free atmosphere before its further use. The chemical formula of polyaniline is shown in Figure 1.

### Characterization of polyaniline

#### XRD analysis

The crystal phase and structure of NPA was determined by X-ray diffractometer (XRD, BRUKER D8) equipped with Cu target for generating Cu,  $K_\alpha$  radiation ( $\lambda = 0.15406 \text{ nm}$ ). The accelerating voltage and the applied current were 40 KV and 30 mA, respectively. The instrument was operated under 1 s step scan and  $0.020^\circ$  ( $2\theta$ ) over  $4$  to  $64^\circ$ . Crystallite size (D) of NPA was calculated by Debye Scherer Equation:

$$D = k \times \lambda / \beta \times \cos \theta \quad (1)$$

Where, k is shape factor equal to 0.89,  $\theta$  is the Bragg's diffraction angle,  $\Delta$  is full width at half maximum (FWHM) in radians for the most intense diffraction peak.,  $\lambda$  is X-ray wavelength (0.15406 nm) for Cu target  $K_\alpha$  is radiation (Srinivas et al., 2012).

#### UV-visible absorption study

To determine the absorption edge of synthesized NPA powder, UV-visible spectra of its 100 mg/L suspension in 1 M HCl was recorded over 200 to 800 nm on a spectrophotometer (SANYO, SP65). Band gap energy ( $E_g$ ) of NPA was calculated as follow:

$$E_g = 1240/\lambda \quad (2)$$

Where,  $\lambda$  is absorption edge wavelength in nm.

To determine bond structure of NPA, its 10 mg powder was mixed with one gram KBr and pressed to get a transparent disc in a moisture-free atmosphere. Spectra was recorded over 400 to 4000  $\text{cm}^{-1}$  on a FTIR spectrometer (FTIR-65, Perkin-Elmer).

#### Photocatalytic activity

Aqueous solution (100 ml) of phenol of known initial concentration was mixed with specified amount (typically 20 mg) of NPA in a batch type reactor described previously (Alebel et al., 2015). The suspension was stirred using magnetic stirrer in dark condition for 30 min to establish adsorption-desorption equilibrium between the photocatalyst and the phenol. The reaction mixture was then exposed to radiation ( $\lambda = 420 \text{ nm}$ ) from a xenon lamp (300 W, PLS-SXE300, Trusttech Co. Ltd., Beijing, intensity: 700  $\text{mW cm}^{-2}$ ) kept 20 cm above the reactor tube. Oxygen gas was bubbled through the reaction mixture at 100 ml/min.

As the reaction proceeded, 5 mL suspension was taken out at regular interval, centrifuged at 6000 rpm for 10 min and filtered through 0.22 mm pore size filter paper. Absorption of clear filtrate was recorded at  $\lambda = 600 \text{ nm}$ . Percent degradation (R) was calculated with the relation:

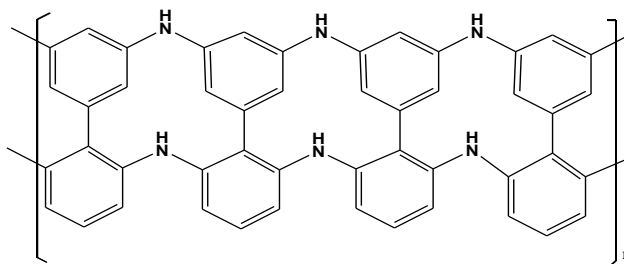


Figure 1. Polyaniline molecular structure.

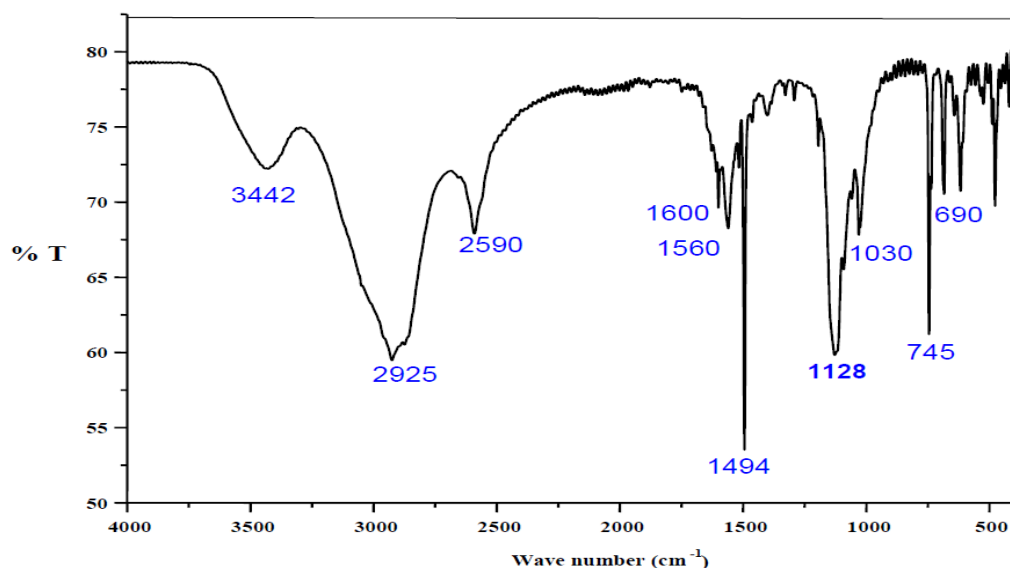


Figure 2. XRD pattern of as-synthesized polyaniline.

$$R = [(A_0 - A_t) / A_0] \times 100 \quad (3)$$

Where,  $A_0$  and  $A_t$  are absorptions at initial stage and at time  $t$ , respectively.

## RESULTS AND DISCUSSION

### X-ray diffraction (XRD) study

XRD pattern of NPA is exhibited in Figure 2. The observed most intense diffraction peak at  $2\theta = 21.254^\circ$  are due to planes of benzenoid and quinoid rings. Shukla et al. (2010) has reported a profile similar to that of NPA in the same synthetic routes. Crystallite size ( $D$ ) of NPA calculated from Debye Scherer formula, described previously was 37 nm. The observed XRD pattern of NPA reveals aniline hydrochloride ( $C_6H_8ClN$ ) with monoclinic structure. However, Srinivas et al. (2012) have reported that XRD pattern of NPA generally differs because of synthetic routes (chemical polymerization, electric polymerization, co-polymerization and plasma-polymerization)

followed and solvent (HCl,  $CH_3O$ , etc.) used.

### UV-visible absorption study

The UV-visible absorption spectra of synthesized NPA are presented in Figure 3. The absorption peaks observed at 328 and 631 nm are due to  $\pi-\pi^*$  transition of benzenoid rings and absorption of the quinoid rings, respectively (Shukla et al., 2010) confirm the NPA emeraldine (aniline hydrochloride). Using the absorption edge wavelength as 631 the band gap energy of NPA was obtained as 1.96 eV which falls well within the visible region of electromagnetic radiation.

### FTIR spectroscopic study

Fourier transform infra-red (FTIR) spectra of synthesized polyaniline (NPA) emeraldine salt is shown in Figure 4. The observed absorption frequencies and the

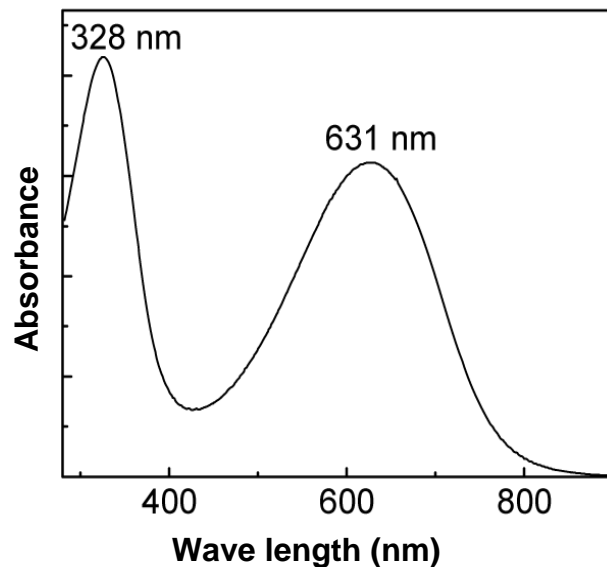


Figure 3. UV-visible absorption Spectra of NPA, in 1 M HCl.

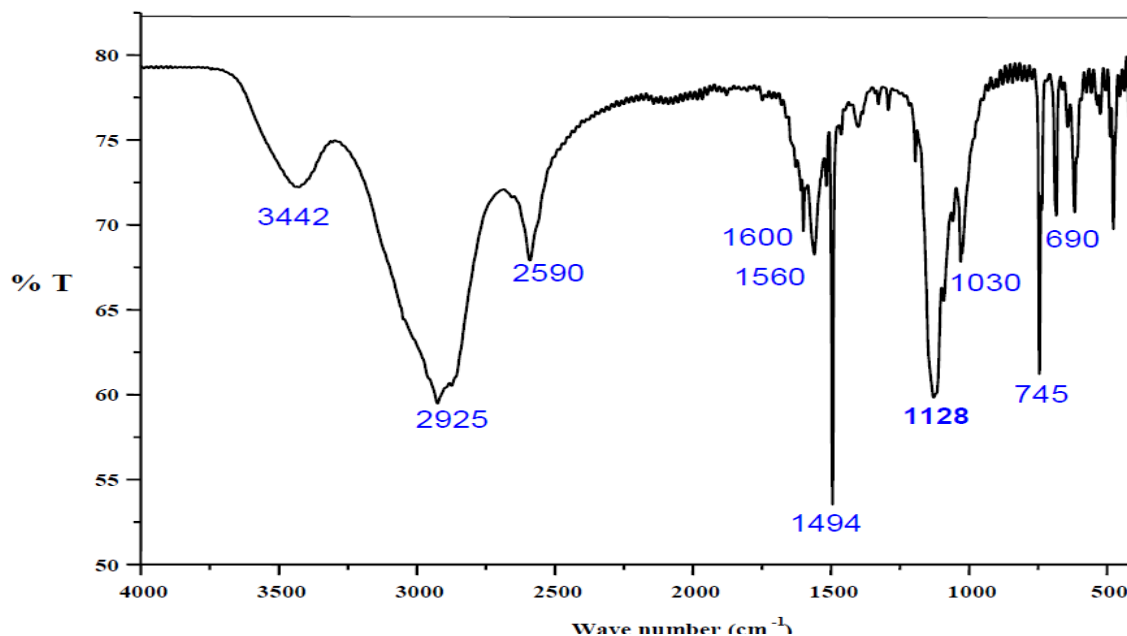


Figure 4. FTIR Spectra of as-synthesize NPA.

corresponding functional group associated with them are listed in Table 1. The recorded FTIR spectra of NPA matched with those reported by Tang et al. (1988) and Vivekanandan et al. (2011). The band observed at  $3442\text{ cm}^{-1}$  is due to N-H stretching and at  $2925\text{ cm}^{-1}$  from C-H stretching. The absorption peak observed at  $1600\text{ cm}^{-1}$  is attributed to C=C stretching in aromatic nuclei and at  $1560\text{ cm}^{-1}$  is due to C=N stretching quinoid. Absorption band at  $1494\text{ cm}^{-1}$  evidenced to C=N stretching in aromatic compounds. Further, absorption at  $1128\text{ cm}^{-1}$  is

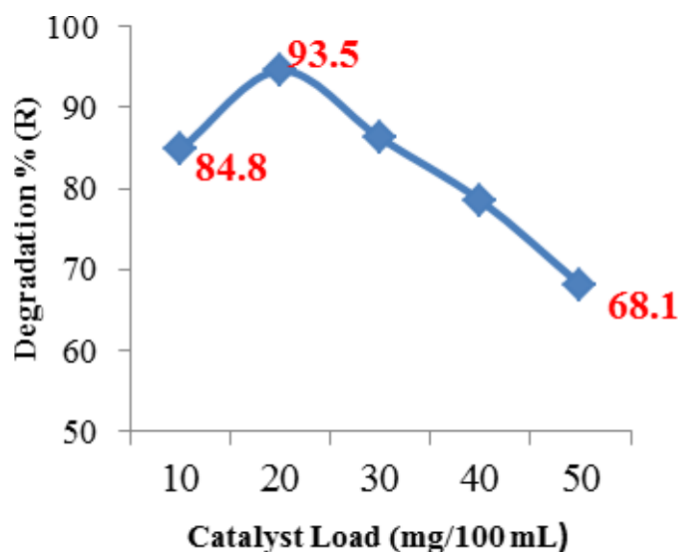
from C-H bending vibrations. The remaining peaks at  $1030/690$  and  $745\text{ cm}^{-1}$  are characteristic of C-C aromatic ring and C-H out of plane bending, respectively.

#### Photo-catalytic degradation study

Photo-catalytic activity of NPA was tested following degradation of phenol in aqueous solution. Effects of parameters such as photo-catalyst load, pH of reaction

**Table 1.** FTIR absorption frequencies and corresponding functional group.

$\nu(\text{cm}^{-1})$	Expected vibrations
3442	N-H stretching
2925	C-H stretching bonding
1600	C=C stretching aromatic Benzenoid rings
1494	C=N stretching Benzenoid rings
1128	C-H bending vibration
1560	C=N stretching in Quinoid rings
1030 and 690	C-C Aromatic ring deformation
745	C-H out of plane bending

**Figure 5.** Plot of percent degradation of phenol at 180 min as a function of NPA load (phenol initial concentration  $50 \text{ mg.L}^{-1}$  and  $\text{pH}=10$ ).

media and substrate initial concentration on the degradation of phenol have been investigated.

#### **Effect of photo-catalyst load**

Plot of percent degradation of phenol at 180 min, as a function of NPA load using fixed initial concentration of phenol and pH, is presented in Figure 5.

Maximum degradation of phenol (93.5%) was observed at optimum photocatalyst load ( $200 \text{ mg.L}^{-1}$ ). The observed lower degradation of phenol, using catalyst amount less than the optimum load, may be due to availability of fewer photo-catalyst active sites per substrate (phenol) molecule for photo-excitation. Further, the reason for diminished phenol degradation at higher catalyst load than the optimum value may be (a) decrease in specific surface area of the photo-catalyst due to agglomeration,

therefore, availability of fewer active sites at photo-catalyst surface and (b) diminished penetration of photons to the photo-catalyst surface, due to the screening effect and enhanced light scattering (Goncalves et al., 1999).

#### **Effect of pH**

Plot of percent degradation of phenol at 180 min as a function of pH at fixed initial phenol concentration and catalyst load is shown in Figure 6. The desired initial pH of the reaction mixture was maintained using 0.1 M HCl or 0.1 M NaOH solution. Degradation of phenol gradually increases on raising pH from 3 to 10 and then it decreases at higher pH. Least degradation at the lowest studied pH 3 may be due to the competitive adsorption at the photo-catalyst surface of hydrogen ions ( $\text{H}^+$ ) and

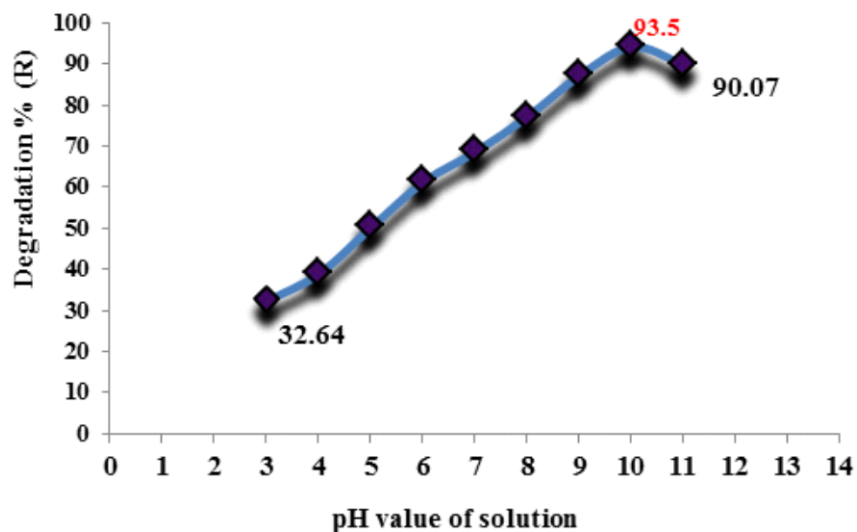


**Figure 6.** Plot of percent degradation of phenol at 180 min as a function of pH [catalyst load = 200 mg.L<sup>-1</sup> and phenol initial concentration = 50 mg.L<sup>-1</sup>].

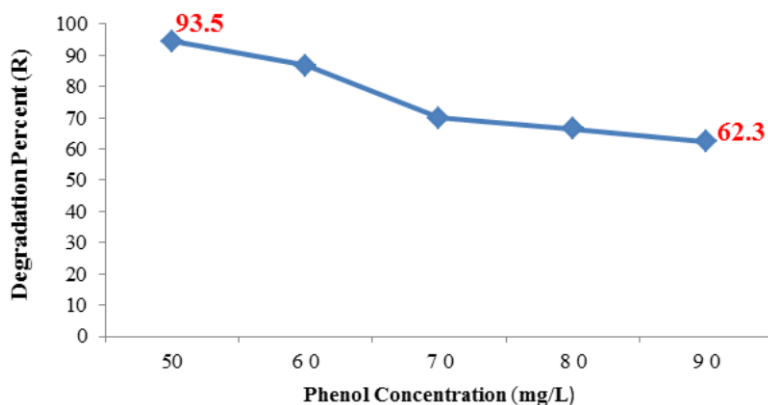


**Figure 7.** Plot of percent degradation of phenol at 180 min as a function of its initial concentration (catalyst load: 200 mg L<sup>-1</sup> and pH: 10).

similarly charged protonated phenol molecules. As the pH increases from 3 to 10 the OH<sup>-</sup> to H<sup>+</sup> ratio gradually increases which facilitates the availability of increased number of hydroxyl (OH<sup>-</sup>) ions required for the formation of photo-catalytic reactive hydroxyl (<sup>•</sup>OH) radicals. Lowering of phenol degradation rate above pH 10 may be attributed to ion-ion repulsion of negatively charged phenoxide and the deprotonated photo-catalyst surface.

#### **Effect of phenol initial concentrations**

Plot of percent degradation of phenol at 180 min as a function of its initial concentration (using fixed catalyst load 200 mg L<sup>-1</sup> and pH 10) is presented in Figure 7. Degradation of phenol decreases with increasing initial

concentration of phenol. This may be because with increasing phenol initial concentration (a) availability of active sites per substrate (phenol) molecule at the photo-catalyst surface decreases and (b) number of photons reaching at the catalyst surface is lowered.

#### **Effects of catalyst and visible light**

Figure 8 depicts percent degradation of phenol as a function of time under (a) visible light without catalyst (b) no light with catalyst and (c) under visible light with catalyst are presented in Figure 8. Using phenol initial concentration, 50 mg L<sup>-1</sup>, optimum catalyst load 200 mg L<sup>-1</sup> and pH 10, degradation of phenol at 180 min were 2.35, 18.08 and 93.5%, respectively. It shows that catalyst and

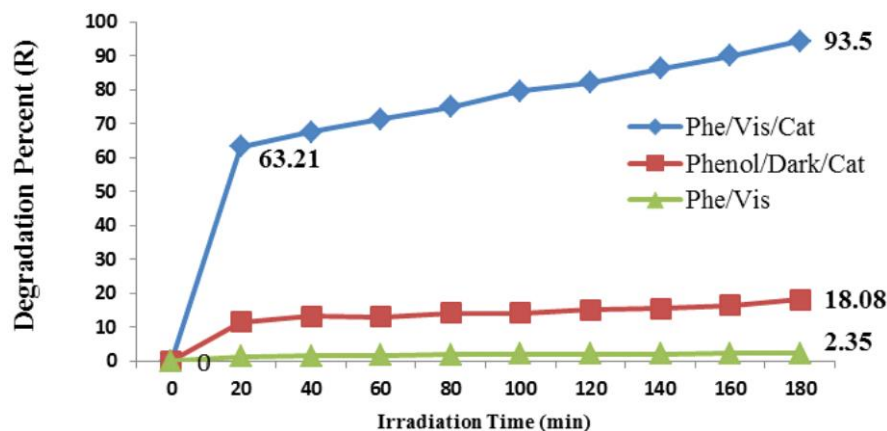


**Figure 8.** Percent degradation of phenol as a function of time under (a) visible light without catalyst (b) no light (darkness) with catalyst and (c) under visible light with catalyst (phenol initial Concentration  $50 \text{ mg L}^{-1}$ , optimum catalyst load  $200 \text{ mgL}^{-1}$  and pH 10).

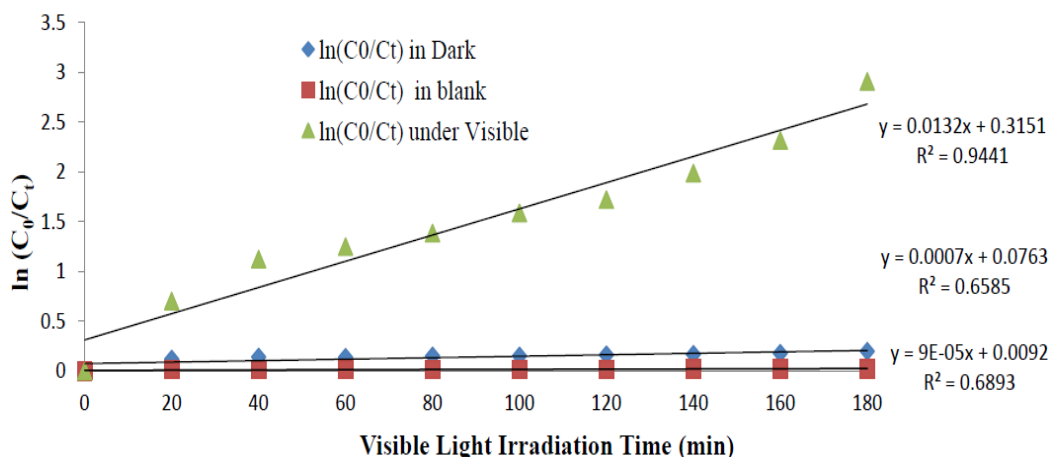


**Figure 9.** Plots of  $\ln C_0/C_t$  as a function of reaction time under (a) visible light without catalyst (b) no light (darkness) with catalyst (NPA) and (c) under visible light with catalyst (phenol initial concentration  $50 \text{ mgL}^{-1}$ , optimum catalyst load  $200 \text{ mgL}^{-1}$  and pH 10).

irradiation have cumulative effect for enhancing the degradation of the phenol; however, the catalytic effect dominates over photolytic contribution.

### Kinetic study of photo-catalytic

#### Degradation

Photo-catalytic degradation of phenol follows first order kinetics represented by the relation.

$$kxt = \ln(C_0/C_t) \quad (4)$$

Where,  $k$  is reaction rate constant in  $\text{min}^{-1}$ ,  $C_0$  and  $C_t$  are concentrations of phenol at initial stage and at time 't',

respectively.

Using phenol initial concentration  $50 \text{ mgL}^{-1}$ , optimum catalyst load  $200 \text{ mgL}^{-1}$  and pH 10, plots of  $\ln C_0/C_t$  as a function of reaction time under (a) visible light without catalyst (b) no light with catalyst and (c) under visible light with catalyst are linear (Figure 9). Under the above reaction conditions phenol degradation rate constants were:  $1.31 \times 10^{-4}$ ,  $1.11 \times 10^{-3}$  and  $1.62 \times 10^{-2} \text{ min}^{-1}$ , respectively.

#### Mechanism of phenol photo-catalytic degradation

NPA acts as either an electron donor or an acceptor for molecules in its surrounding medium. Degradation of phenol over NPA surface is initiated by the absorption of a

**Table 2.** Aqueous Phenol Degradation Mechanisms on NPA Photocatalyst.

NPA + hv	→	$e^-_{cb} + h^+_{vb}$	Step-I
$h^+_{tr} + e^-_{tr}$	→	$e^-_{cb} + \text{heat}$	Step-II
$4h^+ + 2H_2O$	→	$\cdot OH + 4H^+$	Step-III
$h^+ + OH^-$	→	$\cdot OH$	Step-IV
$e^- + O_2$	→	$O_2^-$	Step-V
$O_2^- + 2H^+$	→	$H_2O_2$	Step-VI
$H_2O_2$	→	$2\cdot OH$	Step-VII
Phenol + $\cdot OH$	→	$CO_2 + H_2O$	Step-VIII

photon with energy equal or more than its band gap energy (1.96 eV) producing electron-hole ( $e^-h^+$ ) pairs (Step 1). The hole ( $h^+_{vb}$ ) at the valence band is strongly oxidizing and the electron ( $e^-_{cb}$ ) at the conduction band is strongly reducing. The electron-hole pair may either recombine to produce heat (Step II) or may involve in the subsequent redox reactions. The hole ( $h^+$ ) reacts with  $H_2O$  molecule or hydroxide ( $OH^-$ ) ion to generate  $\cdot OH$  radicals (Step-III and Step-IV). Photo-excited electron at the conduction band interacts with the surface-adsorbed oxygen and  $H^+$  ion generating hydroxy radicals ( $\cdot OH$ ) (Steps V to VII). The  $\cdot OH$  radicals being strong oxidants, finally, degrade the substrate (phenol) molecules to  $CO_2 + H_2O$  (Step VIII) (Umar and Abdullah, 2008; Liotta et al., 2009) (Table 2).

## Conclusions

NPA has been synthesized by chemical oxidative polymerization of aniline. XRD analysis revealed that NPA has crystal size 37 nm with monoclinic structure. Due to its high charge separation efficiency and low band gap energy (1.96 eV) NPA has proved an efficient photocatalyst for phenol degradation, a serious water pollutant. Using phenol initial conc. ( $50 \text{ mg L}^{-1}$ ), as high as 93.5% phenol degradation could be achieved at optimum NPA load ( $200 \text{ mgL}^{-1}$ ) and pH = 10. Therefore, NPA may be a promising material for a clean, cost-effective and efficient large scale treatment of water contaminated with phenol.

## Conflict of Interests

The authors have not declared any conflict of interests.

## ACKNOWLEDGEMENT

Authors are grateful to Ethiopian MOE for financial support for carrying out this work. The valuable support from Haramaya University Research Laboratory, Addis Ababa University Chemistry Research Lab and Ethiopian Geological Survey Research Laboratory (particularly,

Geosciences Lab Directorate) are thankfully acknowledged.

## REFERENCES

- Achamo T, Yadav OP (2016). Removal of 4-Nitrophenol from Water Using Ag–N–P-Tridoped  $TiO_2$  by Photocatalytic Oxidation Technique. *Anal. Chem. Insights* 11:29-34.
- Alebel N, Yadav OP, Isabel D, Abi MT (2015). Cr-N Co-doped ZnO Nanoparticles: Synthesis, Characterization and Photocatalytic Activity for Degradation of Thymol Blue. *Bull. Chem. Soc. Ethiop.* 29(2):247-258.
- Arjunan B, Karuppan M (2011). Degradation of phenol in aqueous solution by fenton, Sono-Fenton and Sono-photo-Fenton Methods *CLEAN– Soil Air Water* 39:142-147.
- Ali H, Gemeay G, Rehab ESh, Mansour AI, Zaki AB (2007). Preparation and Characterization of NPA- $MnO_2$  Composites and their Catalytic Activity. *J. Colloid Interface Sci.* 308(1):385-394.
- Azni I, Katayon S (2002). Degradation of Phenol in Wastewater using Anolyte Produced from Electrochemical Generation of Brine Solution. *Global Nest: Int. J.* 4(2-3):139-1344.
- Bak T, Nowotny J, Rekas M, Sorrell CC (2002). Photo-electrochemical generation of hydrogen from water using solar energy. Materials-related aspects. *Int. J. Hydrogen Energy* 27(4):1022–2791.
- Basha K, Mahammediyas B, Rajendran A, Thangavelu V (2010). Recent advances in the biodegradation of phenol: A review. *Asian J. Exp. Biol. Sci.* 1(3):219-234.
- Goncalves MST, Oliveira-Campos FMA, Pinto SMM, Plasencia SMP, Queiroz PR (1999). Photochemical treatment of solutions of azo dyes containing  $TiO_2$ . *Chemosphere*, 39(5):781-786.
- Gospodinova N, Terlemezyan L (1998). Conducting Polymers Prepared by Oxidative Polymerization. *Polyaniline Program. Polym. Sci.* 23(1):1443–1484.
- Guido B, Silvia B, Carlo R, Laura A (2008). Technologies for the Removal of Phenol from fluid Streams: A Short Review of Recent Developments. *J. Hazard. Mater.* 160(4):265–288.
- Hirotsugu K, Hiromasa G (2011). Preparation and Properties of Polyaniline in the Presence of Trehalose. *Soft Nanosci. Lett.* 1:71-75.
- Khazi MB, Aravindan R, Viruthagiri Th (2010). Recent Advances in the Biodegradation of Phenol: A Rev. *Asian J. Exp. Biol. Sci.* 1(2):219-234.
- Kiros G, Yadav OP, Abi MT (2013). Effect of Ag-N co-doping in Nanosize  $TiO_2$  on Photocatalytic Degradation of Methyl Orange Dye. *J. Surf. Sci. Technol.* 29:1-14.
- Liotta LF, Gruttadauria M, Carlo GD, Perrini G, Librando V (2009). "Heterogeneous catalytic Degradation of Phenolic Substrates". *J. Hazard. Mater.* 162(3):588-606.
- Marshet G, Yadav OP, Abi T, Jain DVS (2015). Effect on Photo-Catalytic Activity of Zinc Oxide Nanoparticles upon Doping with Silver and Sulphur in Degradation Reaction of Malachite Green. *J. Surf. Sci. Technol.* 31(1-2):69-76.
- Mohammad D, Ayati B, Ganjidoust H, Sanjabi S (2012). Kinetics Study of Photocatalytic Process for Treatment of Phenolic Wastewater by

- TiO<sub>2</sub> Nanopowder Immobilized on Concrete Surfaces. *Toxicol. Environ. Chem.* 94(6):1086-1098.
- Salaices M, Serrano B, de Lasa HI (2004). Photocatalytic Conversion of Phenolic Compounds in Slurry Reactors". *Chem. Eng. Sci.* 59(1):3-15.
- Shawabkeh RA, Chessman OA, Bisharat GI (2010). Photocatalytic Degradation of Phenol using Fe-TiO<sub>2</sub> by Different Illumination Sources. *Int. J. Chem.* 2(2):10-18.
- Shukla SK, Bharadvaja A, Tiwari A, Parashar GK, Dubey GC (2010). Synthesis and characterization of Highly Crystalline Polyaniline Film Promising for Humid Sensor. *Adv. Mater. Lett.* 1(2):129-134.
- Srinivas CH, Srinivasu D, Kavitha B, Narsimlu N, Siva Kumar K (2012). Synthesis and Characterization of Nanosized Conducting Polyaniline. *J. Appl. Phys.* 1(5):12-15.
- Sun H, Feng X, Wang S, Ang HM, Tade MO (2011). Combination of adsorption, photochemical and photocatalytic degradation of phenol solution over supported zinc oxide: Effects of support and sulphate oxidant. *Chem. Eng. J.* 170:270-277.
- Tang J, Jing X, Wang B, Wang F (1988). Infrared Spectra of Soluble Polyaniline. *Synth. Met.* 24(3):231-238.
- Tesfay W, Yadav O, AbiTadesse P, Kaushal J (2013). Synthesis, characterization and photocatalytic activities of Ag-N- co-doped ZnO Nanoparticles for Degradation of Methyl Red Dye. *Bull. Chem. Soc. Ethiop.* 27(2):221-232.
- Tao Y, Cheng ZL, Ting KE, Yin XJ (2012). Photocatalytic Degradation of Phenol Using Nanocatalyst: Mechanism and Kinetics. *J. Catal.* 2013, Article ID 364275, 6 pages <http://dx.doi.org/10.1155/2013/364275>.
- Umar IG, Abdullah AH (2008). Heterogeneous Photocatalytic Degradation of Organic Contaminants over Titanium Dioxide: A review of fundamentals, progress and problems. *J. Photochem. Photobiol. C: Photochem. Rev.* 9(1):1-12.
- Vivekanandan J, Ponnusamy V, Mahudeswaran A, Vijayanand PS (2011). Synthesis, Characterization and conductivity study of polyaniline prepared by chemical oxidative and electrochemical methods. *Arch. Appl. Sci. Res.* 3(6):147-153.
- Yan L, Sun D (2007). Development of Fe<sub>2</sub>O<sub>3</sub>-CeO<sub>2</sub>-TiO<sub>2</sub>/γ-Al<sub>2</sub>O<sub>3</sub> as catalyst for catalytic wet air oxidation of methyl orange azo dye under room condition. *Appl. Catal. B: Environ.* 72(8):205-211.